Int. J. Solids Structures, 1977, Vol. 13, pp. 337–355. Pergamon Press. Printed in Great Britain

CREEP BUCKLING AND POSTBUCKLING OF CIRCULAR CYLINDRICAL SHELLS UNDER AXIAL COMPRESSION†

HANS OBRECHT
Division of Engineering and Applied Physics, Harvard University, Cambridge, MA 02138, U.S A.

(*Received* 16 *April* 1976)

Abstract—An infinitely long, axially compressed, circular cylindrical shell with an imperfection in the shape of the axisymmetric classical buckling mode, undergoing steady or non-steady creep, is analyzed. The axisymmetric problem is solved incrementally using nonlinear shell equations The ratio of the applied stress to the classical buckling stress determines if the shell will collapse axisymmetrically or if it will bifurcate into a nonaxisymmetric mode, and whether or not bifurcation will result in instantaneous collapse. The bifurcation problem is formulated exactly and the initial postbuckling behavior is investigated via an asymptotic elastic analysis, based on Koiter's general theory Numerical results are compared with available experimental data.

NOTATION

E	Young's modulus
ν	Poisson's ratio (taken as 1/3)
R	cylinder radius
h	wall thickness
X, Y	axial and circumferential coordinates
c	$=[3(1-\nu^2)]^{1/2}$
q_0	$=(2cR/h)^{1/2}$
U, V, W	axial, circumferential and radial displacements
$\bar{W}$	initial radial displacement (imperfection)
Φ_α	rotation of middle surface ($\alpha = 1, 2$)
$E_{\alpha\beta}$	middle surface strains ($\beta = 1, 2$)
$\kappa_{\alpha\beta}$	bending strains
σ	average axial stress
τ_{ij}	stress tensor ($i, j = 1, 2, 3$)
S_{ij}	stress deviator ($= \tau_{ij} - \frac{1}{3}\tau_{kk}\delta_{ij}$)
J_2	$=\frac{1}{2}S_{ij}S_{ij}$
$M_{\alpha\beta}$	bending moments
$N_{\alpha\beta}$	stress resultants
Q_α	transverse shear forces
η_{ij}^e	elastic strains
η_{ij}^c	creep strains
e_c	$=\sqrt{\frac{1}{2}\eta_{ij}^c\eta_{ij}^c}$
η_{ij}	total strains ($= \eta_{ij}^e + \eta_{ij}^c$)
ϵ_c	uniaxial creep strain
F	Airy stress function
t	time
$C_{\alpha\beta}^{(i)}$	creep terms (eqn 12)
x	$= Xq_0/R$
y	$= Yq_0/R$
w	$= W/R$
$\bar{w}$	$= \bar{W}/h$
u	$= Uq_0/2ch$
v	$= Vq_0/2ch$
ϕ_α	$= \Phi_\alpha q_0/2c$
$e_{\alpha\beta}$	$= E_{\alpha\beta}R/2ch$
$k_{\alpha\beta}$	$= \kappa_{\alpha\beta}R/2c$
σ_{ij}	$= \tau_{ij}R/2cEh$
$m_{\alpha\beta}$	$= M_{\alpha\beta}R/Eh^3$
$n_{\alpha\beta}$	$= N_{\alpha\beta}R/Eh^2$
q_α	$= Q_\alpha R^2/Eh^3q_0$
ϵ_{ij}	$= \eta_{ij}R/2ch$
f	$= Fq_0^2/Eh^2R$
k_n, n, p	creep parameters (eqn 1)
k_m, m	creep parameters (eqn 2)

†This work was supported in part by the Air Force Office of Scientific Research under Grant AFOSR-73-2476, and by the Division of Engineering and Applied Physics, Harvard University.

t_0, t_1, t_2 time scales (eqn 7)
τ $= t/t_0$
σ_{c1} classical elastic buckling stress ($= Eh/cR$)
σ_{cr} critical bifurcation stress of imperfect elastic shell
λ $= \sigma/\sigma_{c1}$
λ_{cr} $= \sigma_{cr}/\sigma_{c1}$
ξ amplitude of buckling displacement
λ_2 postbuckling coefficient (eqn 23)
α postbuckling parameter (eqn 26)
s circumferential wave number
Δ average shortening per unit length
S_0 prebuckling axial stiffness (eqn 25a)
S postbuckling axial stiffness (eqn 25b)

Operators
$()_{,x}$ $= \partial()/\partial x$
$()_{,y}$ $= \partial()/\partial y$
$(\dot{})$ $= \partial()/\partial t$
$\langle\rangle$ denotes average over the cylinder.

INTRODUCTION

Creep buckling, or creep collapse, of circular cylindrical shells is said to occur at a certain critical time when the deformations, or deformation-rates, tend to infinity or exceed prescribed limits. Depending on the applied stress buckling can also occur as the result of bifurcation into a different equilibrium configuration which may, or may not, result in instantaneous loss of load carrying capacity.

In most of the recent investigations of the creep buckling of circular cylinders the shells were presumed to contain axisymmetric or nonaxisymmetric imperfections and the critical times at which the deflections tended to infinity were calculated in a quasi-static manner[1–7]. Hoff[8, 9] has reviewed most of this work.

One of the first attempts to account for bifurcation in an approximate way was made by Samuelson[1]. Hoff[10, 11] has obtained approximate, explicit expressions for the critical bifurcation time by combining his earlier results for a cylinder with an axisymmetric imperfection[2] with the results of Koiter's bifurcation analysis[12] of a similar elastic cylinder.

Apparently Grigoliuk and Lipovtsev (see [13]) were the first to conduct a rigorous bifurcation analysis of shells undergoing creep. Unfortunately their work, which was followed by a number of Russian authors (see [14, 15]), has so far been largely overlooked in the Western literature. They recognized that bifurcation in creep is an instantaneous process which involves creep constitutive terms only insofar as they influence the prebuckling state. They then formulated an exact linear eigenvalue problem for the determination of the critical time at which bifurcation first becomes possible. In [13] they apply this approach to a cylindrical shell with an axisymmetric imperfection under axial compression, and to a perfect cylinder under a radial line load. Similar approaches to bifurcation analysis have been reported by Storåkers[16] and Bushnell[17], who has assembled a general computer code for the analysis of shells of revolution.

In the literature the tacit assumption is usually made that bifurcation will result in instantaneous collapse. Experimental evidence[10, 19] and the results of the following analysis suggest that this need not always be the case.

This investigation is concerned with the creep-buckling behavior of an infinitely long, imperfect circular cylindrical shell under axial compression. Following the work on elastic buckling of Koiter[12] and Budiansky and Hutchinson[20] the imperfection is taken in the shape of the classical axisymmetric buckling mode. Attention is restricted to the case of an "instantaneously" applied load which is subsequently held constant. The critical times at which the shell buckles axisymmetrically or bifurcates into a nonaxisymmetric mode are calculated, and the initial postbuckling behavior is investigated.

Using nonlinear shell equations the axisymmetric prebuckling problem is cast in incremental form and solved numerically for steady as well as nonsteady creep constitutive properties. A typical plot of the time-dependence of, say, the maximum radial displacement is given in Fig. 1. The fundamental axisymmetric path (curve A) shows the instantaneous elastic contribution (w_e) and the growth of the deflections due to creep. For nonlinear creep constitutive laws a finite critical time τ_a usually exists, in the neighborhood of which the displacements increase very

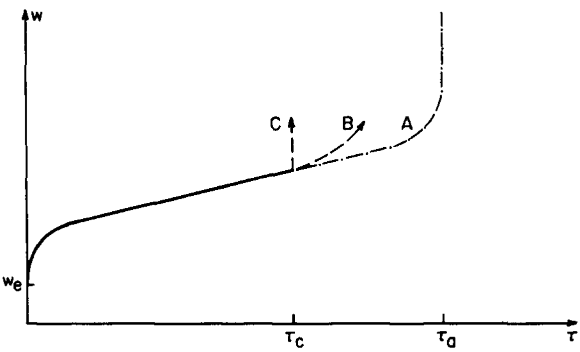

Fig. 1. Typical plot of time dependence of the radial displacement w.

rapidly. The growth of deflections is accompanied by an increase in circumferential stresses which may bring about nonaxisymmetric bifurcation at the critical bifurcation time $\tau_c \leq \tau_a$.

The bifurcation problem is formulated by making a standard perturbation expansion which leads to an eigenvalue problem for the buckling mode and the associated eigenvalue τ_c. The initial postbuckling stiffness is calculated via an asymptotic, quasi-static analysis which is based on Koiter's general theory of initial postbuckling behavior[21]. The analysis reveals the stability of the shell at the instant of bifurcation. If it is found to be unstable, dynamic snapping will occur (as represented schematically by curve C in Fig. 1). If it is found to be stable then, initially at least, the buckling shell still retains some load-carrying capacity and will continue to creep quasi-statically (curve B).

Figure 2 gives an overview of the outcome of the analysis given in the following sections and summarizes the numerical results for a particular case of steady power law creep. The ordinate is the applied stress σ divided by the elastic bifurcation stress σ_{cr} of the imperfect shell. The abscissa is σ_{cr} normalized by the elastic classical buckling stress σ_{c1} of the perfect shell. Each curve in Fig. 2 corresponds to a constant value of nondimensional critical time τ (which, as well as further details, will be defined later). In Region I the shell does not bifurcate but buckles axisymmetrically. In II it bifurcates nonaxisymmetrically at time τ with stable initial postbuckling behavior, whereas in III the postbifurcation behavior is unstable and at time τ snapping occurs simultaneously with bifurcation.

The analysis is followed by a review of available experimental results, particularly with respect to the nature of buckling, and a comparison with the numerical results is made.

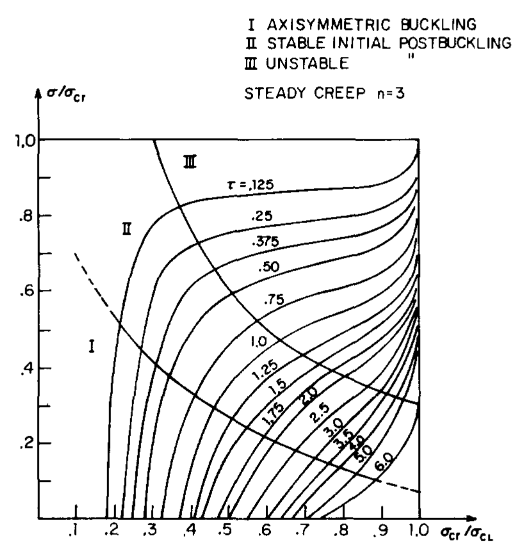

Fig. 2. Critical times and initial postbuckling behavior as a function of the applied stress and the elastic buckling stress.

CONSTITUTIVE RELATIONS

In this study a uniaxial creep law of the power-law strain-hardening type[22] is chosen

$$\dot{\epsilon}_c = k_n \sigma^n \epsilon_c^{1-p} \quad (n > p \geq 1) \tag{1}$$

The dot represents differentiation with respect to time, the subscript c denotes creep and the temperature-dependent material parameters, k_n, n, p are assumed constant. For $p = 1$, (1) reduces to Norton's secondary creep law. A small-strain generalization of (1) is

$$\dot{\eta}_{ij}^c = \Phi_c S_{ij} \tag{2}$$

where in this case $\Phi_c = k_m J_2^m e_c^{1-p}$. In (2) $\dot{\eta}_{ij}^c$ is the creep strain-rate tensor, S_{ij} the stress deviator, J_2 the second invariant of S_{ij} and e_c the second invariant of the accumulated creep strain η_{ij}^c. Note that (2) implies incompressibility and isotropy. Reduction of (2) to the uniaxial case (1) gives the relations between the corresponding parameters, i.e. $m = \frac{1}{2}(n-1)$ and $k_m = k_n 3^{m+1} 2^{-(1+p)/2}$.

Only elastic and creep strains are considered. The total strain rate can then be written in the following form

$$\dot{\eta}_{ij} = \mathcal{M}_{ijkl} \dot{\tau}_{kl} + \Phi_{ijkl} \tau_{kl}. \tag{3a}$$

Inversion yields

$$\dot{\tau}_{ij} = \mathcal{L}_{ijkl} \dot{\eta}_{kl} - \psi_{ijkl} \tau_{kl}. \tag{3b}$$

In (3) $\mathcal{L}_{ijkl}$ and $\mathcal{M}_{ijkl}$ are the tensors of the elastic moduli and compliances. The tensors of the creep terms are simply

$$\left.\begin{aligned} \Phi_{ijkl} &= \Phi_c \left[\frac{1}{2}(\delta_{ik}\delta_{jl} + \delta_{il}\delta_{jk}) - \frac{1}{3}\delta_{kl}\delta_{ij} \right] \\ \psi_{ijkl} &= \mathcal{L}_{ijmn} \Phi_{mnkl} \end{aligned}\right\} \tag{3c}$$

All fourth order tensors are symmetric in the following indices $A_{ijkl} = A_{jikl} = A_{klij}$.

Two-dimensional constitutive relations consistent with first order shell theory are obtained by the usual assumption of a state of approximate plane stress at each point through the thickness. This is equivalent to requiring that transverse shear strains vanish, i.e. $\eta_{\alpha 3} = 0$ $(\alpha = 1, 2)$, and that the contribution of the stress perpendicular to the middle surface make only a negligible contribution to the internal energy, i.e. $\tau_{33} = 0$. Thus from (3b)

$$\dot{\tau}_{\alpha\beta} = \hat{\mathcal{L}}_{\alpha\beta\gamma\delta} \dot{\eta}_{\gamma\delta} - \hat{\psi}_{\alpha\beta\gamma\delta} \tau_{\gamma\delta} \tag{4a}$$

where[23]

$$\hat{\mathcal{L}}_{\alpha\beta\gamma\delta} = \mathcal{L}_{\alpha\beta\gamma\delta} - \frac{\mathcal{L}_{\alpha\beta 33}\mathcal{L}_{33\gamma\delta}}{\mathcal{L}_{3333}}; \quad \hat{\psi}_{\alpha\beta\gamma\delta} = \psi_{\alpha\beta\gamma\delta} - \frac{\mathcal{L}_{\alpha\beta 33}\psi_{33\gamma\delta}}{\mathcal{L}_{3333}}. \tag{4b}$$

Greek indices range only from 1 to 2. Consistent with the above assumptions $e_c^2 = (\eta_{11}^c)^2 + (\eta_{22}^c)^2 + \eta_{11}^c \eta_{22}^c + (\eta_{12}^c)^2$ and J_2 is taken to depend only on the in-plane stresses so that $J_2 = \frac{1}{3}(\tau_{11}^2 + \tau_{22}^2 - \tau_{11}\tau_{22} + 3\tau_{12}^2)$.

INITIAL CREEP INCREMENT

In the case of primary creep, incremental numerical calculations are complicated by the fact that for $t \to 0$, the creep strain-rate (2) becomes infinite. One way of dealing with this problem is to consider a small enough initial time increment δt during which the initial stress state can be assumed to remain constant. Then an analytical expression for the corresponding initial creep increment $\delta\eta_{ij}^c(\delta t)$ can be derived.

Note the identity $\eta_{ij}^c = e_c / J_2^{1/2} S_{ij}$. Differentiation of $e_c = (\frac{1}{2}\eta_{ij}^c \eta_{ij}^c)^{1/2}$ with respect to time and use of (2) gives $\dot{e}_c = k_m J_2^{n/2} e_c^{1-p}$. Assuming a constant J_2, integrating and using the initial condition

$e_c(t=0)=0$ one finds

$$\delta\eta_{ij}^c = (p \cdot k_m)^{1/p} J_2^{(n-p)/2p} S_{ij} \delta t^{1/p}. \tag{5}$$

Together with the initial elastic stress state and a suitably small δt (5) gives starting values for η_{ij}^c and e_c.

TIME SCALE

The critical time depends strongly on the structure, the material properties and the loading conditions. In experiments reported in the literature it has been found to vary from a few minutes to several weeks. The choice of an appropriate time scale is therefore important, particularly for conducting an efficient numerical analysis. In this section three time scales are introduced and an argument is made for one of them.

For a constant stress σ the uniaxial creep law (1) can be integrated directly. Thus the time needed to reach a certain strain ϵ is

$$t = (p \cdot k_n \sigma^n)^{-1} \epsilon^p. \tag{6}$$

If a representative stress σ and the associated strain ϵ can be identified for a given problem then the time resulting from (6) can be used as a reference time.

In the present problem the average axial stress is the natural choice for σ. A particularly useful time scale is the time t_0 needed to reach a strain equal to the elastic strain $\epsilon_e = \sigma/E$, i.e.

$$t_0 = [pK_n E^p \sigma^{n-p}]^{-1}. \tag{7}$$

A different choice is the time t_1 which it takes under a stress σ to reach a strain $\epsilon_{c1} = \sigma_{c1}/E$, where σ_{c1} is the classical elastic buckling stress. With the use of the load-parameter $\lambda(=\sigma/\sigma_{c1})$ which will be used throughout the paper one obtains $t_1 = \lambda^{-p} \cdot t_0$. In Hoff's papers t_1 is called the "Euler time". Finally, setting $\sigma = \sigma_{c1}$ and $\epsilon = \epsilon_{c1}$ in (6) gives $t_2 = \lambda^{n-p} t_0$.

In the limit, as $\lambda \to 0$, critical times normalized by t_2 are found to go to infinity, whereas, if normalized by t_1, they go to zero. In contrast, normalization by t_0 always yielded finite constant values. Also, in the numerical calculations the time increments never had to be chosen larger than unity, and $\tau = t/t_0$ turned out to be the most convenient choice of nondimensional time for the present study.

AXISYMMETRIC RESPONSE

Instantaneous elastic deformations

Consider an infinitely long imperfect circular cylindrical shell under axial compression. The load, which must be smaller than the elastic bifurcation load, is to be applied "instantaneously", but quasi-statically. In the present study it is subsequently held constant, although time-varying loads could be considered without difficulty.

The imperfection is taken in the shape of the classical axisymmetric buckling mode [20]

$$\tilde{w} = -\tilde{\xi} \cos x. \tag{8}$$

Here $\tilde{w}$ is the nondimensional radial displacement associated with the initial deflection, and $\tilde{\xi}$ is the initial imperfection amplitude divided by the shell thickness.

The analysis is made within the context of nonlinear Donnell-Mushtari-Vlasov shell equations [24]. The usefulness of these equations has been questioned on the ground that creep buckling is associated with the development of "large" deflections. As will be seen later, at small imperfection levels, all relevant phenomena take place at deflections which are at most of the order of the thickness, and thus lie well within the range of applicability of the theory.

The shell equations are used in nondimensional form. The notation is identical to the one introduced in [20] and is given in the notation list. In conjunction with the time scales introduced earlier, this nondimensionalization effectively eliminates most material constants, as well as the radius-to-thickness ratio R/h from the equations, leaving only ν, n, p and λ as free parameters.

The initial response of the shell is elastic and with the imperfection shape (8) the nonlinear shell equations can be solved exactly to give [12, 20]

$$\left.\begin{aligned} w_e &= \frac{\nu\lambda}{c} - \xi\left[\frac{\lambda}{1-\lambda}\right]\cos x \\ n_{22}^e &= -\xi\left[\frac{\lambda}{1-\lambda}\right]\cos x \end{aligned}\right\} \tag{9}$$

and similar expressions for the associated stresses, strains and displacements. The subscript (or superscript) e denotes the elastic response at time $t = 0$. Equations (9) are the initial conditions for the creep problem.

Formulation of rate equations

The rate of the approximate two-dimensional strain tensor $\dot{\eta}_{\alpha\beta}$ is given in terms of the rates of the midsurface stretching strain $\dot{E}_{\alpha\beta}$ and bending strain $\dot{\kappa}_{\alpha\beta}$ by

$$\dot{\eta}_{\alpha\beta} = \dot{E}_{\alpha\beta} + z\dot{\kappa}_{\alpha\beta} \quad (\alpha, \beta = 1, 2). \tag{10}$$

In (10) z is measured along the outward normal. The usual definitions for the resultant stress tensor $N_{\alpha\beta}$ and the bending moment tensor $M_{\alpha\beta}$ give

$$\dot{N}_{\alpha\beta} = h\hat{\mathscr{L}}_{\alpha\beta\gamma\delta}\dot{E}_{\gamma\delta} - C_{\alpha\beta}^{(1)} \quad \text{and} \quad \dot{M}_{\alpha\beta} = \frac{h^3}{12}\hat{\mathscr{L}}_{\alpha\beta\gamma\delta}\dot{\kappa}_{\gamma\delta} - C_{\alpha\beta}^{(2)}. \tag{11}$$

Here h is the thickness of the undeformed shell and the creep terms $C_{\alpha\beta}^{(i)}$ are given by

$$C_{\alpha\beta}^{(i)} = \frac{E}{3(1-\nu^2)}\int_{-h/2}^{h/2} \Phi_c\hat{\tau}_{\alpha\beta}z^{(i-1)}\,dz \quad (i = 1, 2) \tag{12}$$

where $\hat{\tau}_{\alpha\beta} = 3(1-\nu)\tau_{\alpha\beta} - (1-2\nu)\tau_{\gamma\gamma}\delta_{\alpha\beta}$.

The formulation of the rate equations is completed by differentiating the appropriate equilibrium and strain-displacement relations [24] with respect to time. As discussed in more detail in [23, 25] the resulting linear incremental equations can be reduced to a set of six first-order differential equations. The advantage of such a formulation is that it involves no differentiation of terms resulting from the constitutive equations. Nondimensionalized and written in matrix notation the equations take the form

$$\dot{Z}_{,x} + A\cdot\dot{Z} = \dot{p} \tag{13}$$

where $\dot{Z} \equiv (\dot{n}_{11}, \dot{q}_1, \dot{m}_{11}, \dot{u}_1, \dot{w}, \dot{\phi}_1)$. The column vector $\dot{p}$ depends on the creep terms (12) and the matrix A is a function of Z.

Due to the symmetry of the problem about $x = \pm n\pi$ $(n = 0, 1, 2, \ldots)$ the analysis can be restricted to the interval $[0, \pi]$. The appropriate boundary conditions at the two end points are $n_{11} = -\lambda/c$, $q_1 = \phi_1 = 0$ and $\dot{n}_{11} = \dot{q}_1 = \dot{\phi}_1 = 0$.

Equation (13), together with the boundary conditions and the initial conditions (9), constitute the full initial-boundary value problem for the axisymmetric response of the shell.

Equation (13) was solved by dividing the distance between 0 and π into N equal intervals, and by replacing the derivative by central finite differences. This leads to a set of linear algebraic equations in the variables $\dot{Z}_{i,m}$ (where i denotes the spatial and m the time stations) which were then solved by a modified version of Potters' method [26]. For more details the reader is referred to reference [25].

The integral terms (12) which appear in the vector $\dot{p}$ (13) were evaluated numerically by dividing the shell wall into M equal intervals and then using Simpson's rule. Trial calculations showed that $N = 28$ and $M = 10$ provided sufficient accuracy.

Time integration was performed simply by advancing the solution from time τ_m to τ_{m+1} according to

$$Z_{i,m+1} = Z_{i,m} + \dot{Z}_{i,m}\,\Delta\tau_m. \tag{14}$$

In regions of rapidly changing $\dot{Z}$ a mid-point Runge-Kutta scheme was used, and $\dot{Z}$ was calculated at $\tau_{m+(1/2)} = \tau_m + \frac{1}{2}\Delta\tau_m$ by quadratically extrapolating the components of $A(Z)$ in (13) to $\tau_{m+(1/2)}$.

Repeated solution of (14) gives the incremental time history of the axisymmetric response (curve A in Fig. 1). In all cases studied the axisymmetric critical time τ_a was finite for nonzero $\bar{\xi}$.

Hoff[2, 8, 9, 11] gave a closed form expression for the critical time τ_a of an infinite cylinder with an axisymmetric imperfection whose wavelength differs only slightly from (8). The expression is derived for steady creep ($n = 3$) on the basis of a double-membrane model, and elastic strains are accounted for by a correction factor. In the present notation and with t_0 (7) as time scale it reads

$$\tau_a = 0.294\left[\frac{1-\lambda}{\lambda}\right]\ln\left[1 + 0.328\left(\frac{1-\lambda}{\bar{\xi}}\right)^2\right]. \tag{15}$$

A comparison with numerical results will be made in a later section.

BUCKLING AND POSTBUCKLING BEHAVIOR

Bifurcation

Initially, as time increases from $\tau = 0$, the fundamental solution is unique. Suppose that at a certain time $\tau_c \le \tau_a$ the shell reaches a state in which this uniqueness is lost. For constitutive laws which involve creep in a manner such as (3b) it can be shown, within the context of Hill's general theory of bifurcation and uniqueness of incremental boundary-value problems[27, 16], that the creep terms in the incremental relationship, i.e. the second term in (3b), do not enter into the bifurcation problem. Thus the bifurcation problem in creep involves viscous terms only insofar as they determine the current state of stress and deformation of the fundamental mode. In the present case it leads to a linear eigenvalue problem for the eigenmode and the associated eigenvalue τ_c. The formulation of the bifurcation problem is given in the following section, together with the asymptotic postbuckling analysis.

Postbuckling

The important question is now whether, following bifurcation, the shell will snap dynamically or whether it will continue to creep quasi-statically. In other words, whether the initial postbuckling behavior is stable or unstable.

The analysis of this aspect of the problem is based on Koiter's general theory of initial postbuckling behavior[12, 21], and the versions of this theory presented by Budiansky and Hutchinson[28] and Fitch[29]. To determine whether or not bifurcation is associated with snapping we examine if, given the state of stress and deformation at bifurcation, the shell is able to support an additional load increment $\Delta\lambda$, which is "instantaneously" (but quasi-statically) applied. Thus we calculate the initial slope of the static load-deflection equilibrium path in the postbuckling regime associated with the additional *elastic* response. If this slope turns out to be zero or negative the creeping shell will not be able to support the constant load and will collapse dynamically (represented schematically by curve C in Fig. 1). If, on the other hand, the initial slope is positive this analysis does not describe the actual behavior of the creeping shell under constant load. It only indicates that it retains the ability to carry the applied load after bifurcation and will, initially at least, continue to creep quasi-statically (represented schematically by curve B in Fig. 1). Thus, the initial slope of the static load-deflection curve, calculated on the basis of additional elastic responses, determines the stability of the creeping shell under constant load at bifurcation. A somewhat similar approach to the creep buckling of imperfect columns was used in [31].

As in [20, 28, 29] the following series representation of the initial postbuckling behavior is used, where the amplitude of the buckling mode ξ is the independent expansion parameter

$$\lambda = \lambda_c + \Delta\lambda \quad (\Delta\lambda/\lambda \ll 1) \tag{16}$$

$$\begin{Bmatrix} w \\ f \end{Bmatrix} = \begin{Bmatrix} w^c \\ \end{Bmatrix} + \begin{Bmatrix} \bar{w}(\Delta\lambda) \\ \bar{f}(\Delta\lambda) \end{Bmatrix} + \xi \begin{Bmatrix} w^{(1)} \\ f^{(1)} \end{Bmatrix} + \xi^2 \begin{Bmatrix} w^{(2)} \\ f^{(2)} \end{Bmatrix} + \cdots \tag{17a}$$

$$\Delta\lambda = \xi\lambda_1 + \xi^2\lambda_2 + \cdots \tag{17b}$$

In (17a) f is the nondimensional Airy stress function. The series for the other variables are analogous [20]. The first column in (17a) represents the quantities of the fundamental state and the subscript (or superscript) c denotes evaluation at τ_c. The variables in the second column are associated with the elastic increment of the fundamental mode due to $\Delta\lambda$. Terms of order ξ are the solution to the bifurcation problem, and terms with superscripts larger than one are higher order contributions.

In general multiple buckling modes $w^{(1)}$ are possible, but in the present case $w^{(1)}$ will be unique apart from an arbitrary amplitude. It is taken to be orthogonal to the higher order terms and normalized in the following way

$$|w^{(1)}|_{\max} = 1 \text{ and } \iint w^{(1)} w^{(j)} \,\mathrm{d}x\,\mathrm{d}y = 0 \quad \text{for } j \neq 1. \tag{18}$$

Since the postbuckling behavior must be independent of the sign of the buckling mode one finds $\lambda_1 = 0$. Then, consistent with the previous discussion, it is the sign of λ_2 which determines the stability of the shell and snap-buckling can be expected at τ_c if $\lambda_2 \leq 0$.

The formulation is completed by representing the barred quantities in (18) by a Taylor series about $\Delta\lambda = 0$, i.e.

$$\begin{Bmatrix} \bar{w} \\ \bar{f} \end{Bmatrix} = \Delta\lambda \begin{Bmatrix} \bar{w}' \\ \bar{f}' \end{Bmatrix}_{\Delta\lambda=0} + \frac{1}{2}(\Delta\lambda)^2 \begin{Bmatrix} \bar{w}'' \\ \bar{f}'' \end{Bmatrix}_{\Delta\lambda=0} + \cdots \tag{19}$$

where primes denote differentiation with respect to $\Delta\lambda$.

Substitution of (17a) and (19) into the complete shell equations [24] and use of elastic constitutive relations except for the terms labeled c results in a sequence of linear Kármán-Donnell-type equations, of which the following are needed in the analysis

$$\left.\begin{aligned} \bar{w}'_{,xxxx} + \bar{f}'_{,xx} + 2\lambda_c \bar{w}'_{,xx} &= -2(w^c + \bar{w})_{,xx} \\ \bar{f}'_{,xxxx} - \bar{w}'_{,xx} &= 0 \end{aligned}\right\} \tag{20}$$

$$\left.\begin{aligned} \nabla^4 w^{(1)} + 2\lambda_c w^{(1)}_{,xx} + f^{(1)}_{,xx} - 2c(w^c + \bar{w})_{,xx} f^{(1)}_{,yy} - 2c n^c_{22} w^{(1)}_{,yy} &= 0 \\ \nabla^4 f^{(1)} - w^{(1)}_{,xx} + 2c(w^c + \bar{w})_{,xx} w^{(1)}_{,yy} &= 0 \end{aligned}\right\} \tag{21}$$

$$\left.\begin{aligned} \nabla^4 w^{(2)} + 2\lambda_c w^{(2)}_{,xx} + f^{(2)}_{,xx} - 2c(w^c + \bar{w})_{,xx} f^{(2)}_{,yy} - 2c n^c_{22} w^{(2)}_{,yy} &= 2c\psi(f^{(1)}, w^{(1)}) \\ \nabla^4 f^{(2)} - w^{(2)}_{,xx} + 2c(w^c + \bar{w})_{,xx} w^{(2)}_{,yy} &= -c\psi(w^{(1)}, w^{(1)}) \end{aligned}\right\} \tag{22}$$

where

$$\psi(P, Q) = P_{,xx}Q_{,yy} + P_{,yy}Q_{,xx} - 2P_{,xy}Q_{,xy}.$$

Equations (21) constitute the homogeneous eigenvalue problem for bifurcation referred to previously, and τ_c is the lowest value for which the associated solutions are nontrivial. The critical bifurcation time τ_c enters implicitly through the critical axial bending strain $-w^c_{,xx}$ and the critical circumferential stress n^c_{22} of the fundamental solution. The same holds for the general buckling problem within the context of Donnell–Mushtari–Vlasov theory. It can be shown [30] that the curvature tensor $-w^c_{,\alpha\beta}$ and the tensor of the stress resultants $n^c_{\alpha\beta}$ are the only quantities of the fundamental state (including the creep deformations) which have an influence on bifurcation. This point will be important in the context of approximate buckling criteria, which will be discussed later.

As mentioned earlier λ_1 vanishes and the general expression for the postbuckling coefficient λ_2 becomes [29, 20]

$$\frac{\lambda^2}{1-\nu^2} = \frac{3}{c} \frac{\langle Q(f^{(2)}, w^{(1)}, w^{(1)}) + 2Q(f^{(1)}, w^{(1)}, w^{(2)})\rangle}{\langle (w^{(1)}_{,x})^2 - 2c(f^{(1)}_{,yy} w^{(1)}_{,x} - f^{(1)}_{,xy} w^{(1)}_{,y})\bar{w}'_{,x} - c\bar{n}'_{22}(w^{(1)}_{,y})^2 \rangle} \tag{23}$$

where

$$Q(L, M, N) = L_{,yy}M_{,x}N_{,x} + L_{,xx}M_{,y}N_{,y} - L_{,xy}(M_{,y}N_{,x} + M_{,x}N_{,y})$$

and $\langle\,\rangle$ represents averaging over the shell.

Postbuckling parameter α

Following[20] a more convenient measure of the change in overall stiffness due to bifurcation is employed. The average axial shortening per unit length is given by

$$\Delta = -\left\langle \frac{\partial U}{\partial X} \right\rangle = -\left\langle E_{11} - \frac{1}{2}W_{,X}^2 - \bar{W}_{,X}W_{,X} \right\rangle. \tag{24}$$

Expansions (17a) and (19) lead to a similar series for Δ. Introduce now the prebuckling axial stiffness S_0 of the shell in the fundamental mode at τ_c

$$S_0 = \frac{1}{E}\left(\frac{d\bar{\sigma}}{d\Delta}\right)_{\tau_c} = \left(c\frac{R}{h}\right)^{-1}(\bar{\Delta}')^{-1} \tag{25a}$$

where $\bar{\sigma} = \Delta\lambda\sigma_{c1}$, and the initial postbuckling stiffness of the buckled shell S, also at τ_c,

$$S = \frac{1}{E}\left(\frac{d\bar{\sigma}}{d\Delta}\right)_{\tau_c} = \left[\frac{1}{S_0} + c\frac{R}{h}\frac{\Delta^{(2)}}{\lambda_2}\right]^{-1}. \tag{25b}$$

The initial postbuckling parameter α is now defined as[20]

$$\alpha = \frac{2}{\pi}\arctan\left(\frac{S}{S_0 - S}\right). \tag{26}$$

Its values range from $+1$ to -1. A graphic interpretation of α is given in the lower half of Fig. 3.

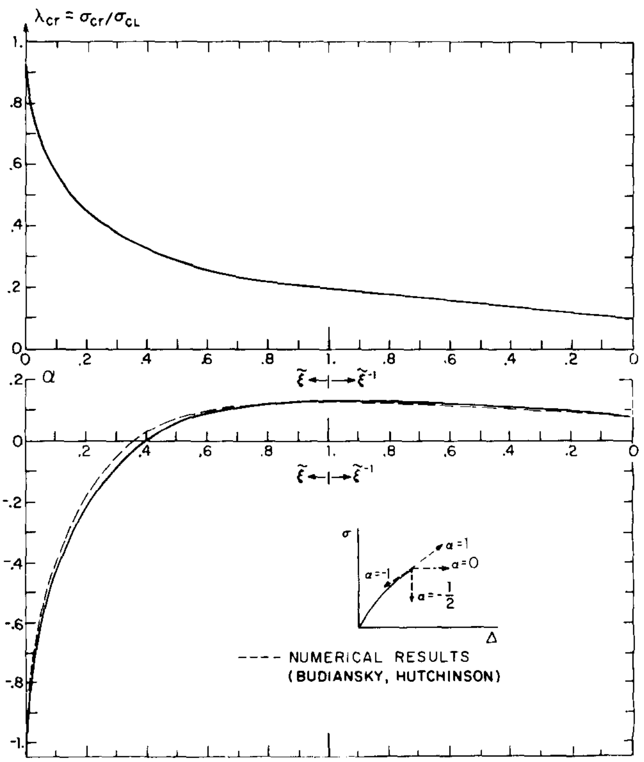

Fig. 3. Buckling and postbuckling of imperfect elastic cylindrical shells under axial compression.

Note that while λ_2 and α do not measure precisely the same characteristics, they always have the same sign.

APPROXIMATE SOLUTION

Equations (20)–(22) will now be solved by first approximating the terms n_{22}^c and $w_{,xx}^c$ and then, following Koiter[12], using a Galerkin procedure.

The numerical calculations showed that throughout the deformation history n_{22} and $w_{,xx}$ remain essentially sinusoidal and that only their amplitudes change with time. To simplify the analysis we use the following approximate representation

$$\left.\begin{aligned} n_{22}(\tau) &= -\bar{\xi}\left[\frac{\lambda}{1-\lambda}\right](1+\eta(\tau))\cos x \\ w_{,xx}(\tau) &= \xi\left[\frac{\lambda}{1-\lambda}\right](1+\omega(\tau))\cos x \end{aligned}\right\}. \tag{27}$$

The functions η and ω depend on time only and account for the effects of creep. For $\tau = 0$ they vanish and eqns (27) reduce to the elastic case (9). Their values can be calculated at each time step from the numerical solution to the axisymmetric problem discussed above. For convenience let

$$\kappa_{xx}^c = -(w^c + \tilde{w})_{,xx} = -K_c \cos x \quad \text{and} \quad n_{22}^c = -n_c \cos x \tag{28}$$

where K_c and n_c follow from (27).

With the use of (27) the solution of (20) is

$$\bar{w}' = -A' \cos x \qquad \bar{f}' = -\frac{y^2}{2c} + A' \cos x \tag{29}$$

where

$$A' = \bar{\xi}\frac{1+\omega_c\lambda_c}{(1-\lambda_c)^2}.$$

The solution of (21) proceeds in a way similar to the one given by Koiter[12]. He considers a buckling pattern of the form

$$w^{(1)} = \sum_{j=1}^{\infty} C_j^{(1)} \cos\left[\frac{1}{2}(2j-1)x\right]\cos sy \tag{30a}$$

and performs the analysis using the full series (30a). His expression for the upper bound to the critical bifurcation stress is then obtained by setting all coefficients $C_j^{(1)}$, except the first, equal to zero. Here we also retain only this first term and, using (18), seek a buckling solution of the form

$$w^{(1)} = \cos\frac{x}{2}\cos sy. \tag{30b}$$

Substitution of (30b) into the compatibility equation of (21) gives a differential equation for $f^{(1)}$ with the following exact solution

$$f^{(1)} = \left(D_1^{(1)}\cos\frac{x}{2} + D_2^{(1)}\cos\frac{3}{2}x\right)\cos sy \tag{30c}$$

where

$$D_1^{(1)} = -\frac{4}{\alpha_0^2}(1-4cs^2K_c); \quad D_2^{(1)} = \frac{16cs^2K_c}{\alpha_2^2}$$

and

$$\alpha_0 = 1+4s^2; \quad \alpha_2 = 9+4s^2.$$

Substitution of (30b,c) into the equilibrium equation and use of a Galerkin procedure gives a condition for bifurcation

$$D = (1-\lambda_c)^2\left[\alpha_0{}^2 + \frac{16}{\alpha_0{}^2} - 8\lambda_c\right] - \tilde{\xi}\Lambda = 0 \tag{31}$$

where

$$\Lambda = 16cs^2\left\{(1-\lambda_c)\left[\lambda_c(1+\eta_c) + \frac{8}{\alpha_0{}^2}(1+\omega_c\lambda_c)\right] - 16cs^2\tilde{\xi}(1+\omega_c\lambda_c)^2\left[\frac{1}{\alpha_0{}^2}+\frac{1}{\alpha_2{}^2}\right]\right\}.$$

For $\omega = \eta = 0$ (31) reduces to an equation which relates the critical bifurcation stress to the imperfection level given by Koiter[12]. In the creep case λ_c is prescribed and D is a function of time τ and the wave number s. The critical time τ_c is the smallest value of τ for which D first vanishes for all possible integer values of $s \cdot q_0$[20]. The actual zeros of D were found by calculating its value at each time step and treating s as a continuous variable, since for thin shells the critical values of sq_0 are large compared to one.

Consider now the limiting case of a perfect shell. (This problem received much attention in the 1950's and 1960's, but the results were not conclusive.) Setting $\tilde{\xi} = 0$ in (31) gives an expression which does not contain creep terms and whose solution is $\lambda_c = 1$ and $s_c = 0.5$ (where s_c is the value that minimizes λ_c). But these are just the critical values for nonsymmetric bifurcation of a perfect elastic shell. This indicates that a perfect shell undergoing creep will not bifurcate at loads below the classical buckling load.

The boundary value problem (22) is again solved approximately using a Galerkin procedure. In [12] Koiter does not consider postbuckling. Details of the following solution procedure are, however, quite similar to those given in [12], so that they need not be repeated here. The functional form of the operators ψ in (22) suggests solutions of the form

$$\left.\begin{aligned} w^{(2)} &= C_{20} + C_{21}\cos x + C_{22}\cos 2x + \cos 2sy\sum_{j=0}^{\infty} C_j^{(2)}\cos jx \\ f^{(2)} &= D_{21}\cos x + D_{22}\cos 2x + \cos 2sy\sum_{j=0}^{\infty} D_j^{(2)}\cos jx \end{aligned}\right\}. \tag{32}$$

In addition to (22) the solutions (32) must satisfy the condition of single-valued circumferential displacement

$$\oint_0^{2R\pi}\left(\frac{\partial V}{\partial Y}\right)\mathrm{d}Y = 0. \tag{33}$$

Substitution of (32) into the compatibility equation of (22) gives an expression relating $C_j^{(2)}$ to $D_j^{(2)}$. Use of this expression, substitution of (32) into the equilibrium equation and again application of the Galerkin procedure leads to linear sets of equations for the coefficients

$$C_{21} + D_{21} = -\frac{cs^2}{4} \tag{34a}$$

$$C_{22} + 4D_{22} = 0 \tag{34b}$$

$$(1-2\lambda_c)C_{21} - D_{21} = \frac{cs^2}{2}(D_1{}^{(1)} + D_2{}^{(1)}) \tag{34c}$$

$$4(2-\lambda_c)C_{22} - 2D_{22} = cs^2D_2{}^{(1)} \tag{34d}$$

$$\sum_{l=-1}^{1}(\alpha_{0,l}C_l^{(2)} + \beta_{0,l}D_l^{(2)}) = -\frac{cs^2}{4} \tag{35a}$$

$$\sum_{l=-1}^{1}(\gamma_{0,l}C_l^{(2)} + \delta_{0,l}D_l^{(2)}) = \frac{cs^2}{2}D_1{}^{(1)} \tag{35b}$$

$$\sum_{l=-1}^{1}[\alpha_{-1,-1+l}C_{-1+l}^{(2)} + \beta_{-1,-1+l}D_{-1+l}^{(2)} + \alpha_{1,1+l}C_{1+l}^{(2)} + \beta_{1,1+l}D_{1+l}^{(2)}] = 0 \tag{35c}$$

$$\sum_{l=-1}^{1}[\gamma_{-1,-1+l}C_{-1+l}^{(2)} + \delta_{-1,-1+l}D_{-1+l}^{(2)} + \gamma_{1,1+l}C_{1+l}^{(2)} + \delta_{1,1+l}D_{1+l}^{(2)}] = 2cs^2D_2{}^{(1)} \tag{35d}$$

$$\sum_{l=-1}^{1} [\alpha_{2,2+l}C_{2+l}^{(2)} + \beta_{2,2+l}D_{2+l}^{(2)}] = 0 \tag{35e}$$

$$\sum_{l=-1}^{1} [\gamma_{2,2+l}C_{2+l}^{(2)} + \delta_{2,2+l}D_{2+l}^{(2)}] = \frac{cs^2}{2}D_2^{(1)} \tag{35f}$$

$$\left.\begin{aligned} &\sum_{l=-1}^{1} [\alpha_{q,q+l}C_{q+l}^{(2)} + \beta_{q,q+l}D_{q+l}^{(2)}] = 0 \qquad (36a)\\ &\sum_{l=-1}^{1} [\gamma_{q,q+l}C_{q+l}^{(2)} + \delta_{q,q+l}D_{q+l}^{(2)}] = 0 \qquad (36b)\end{aligned}\right\} \quad q \geq 3$$

where

$$\begin{aligned} \alpha_{q,q\pm 1} &= -4cs^2K_c & \alpha_{q,q} &= q^2\\ \beta_{q,q\pm 1} &= 0 & \beta_{q,q} &= (q^2+4s^2)^2\\ \gamma_{q,q\pm 1} &= -4cs^2n_c & \gamma_{q,q} &= (q^2+4s^2)^2 - 2\lambda_c q^2\\ \delta_{q,q\pm 1} &= 4cs^2K_c & \delta_{q,q} &= -q^2. \end{aligned}$$

The negative values for l in (35) and (36) result from the products of trigonometric terms in (22). Also, due to the presence of cos $(-x)$ and cos $2x$, as well as constant terms, the cases $q = 0, 1, 2$ need special attention in the Galerkin procedure.

Condition (33) leads to $C_{20} = -(cs^2/4)$ and two equations which are identical to (34a,b).

Equations (36) constitute a banded, infinite system for $C_j^{(2)}, D_j^{(2)}$. By an argument similar to the one given in [12] it can be shown that for $q \to \infty$ eqns (36) reduce to pairs of homogeneous equations with trivial solutions. This provides the justification for truncating the series in (32). Here we set $C_j^{(2)} = D_j^{(2)} = 0$ for $j \geq 3$. The remaining six eqns (35) are then solved numerically by Gaussian elimination.

Now λ_2 can be expressed in terms of the coefficients of $(\bar{w}', \bar{f}')$, $(w^{(1)}, f^{(1)})$ and $(w^{(2)}, f^{(2)})$. We find

$$\frac{\lambda_2}{1-\nu^2} = -\frac{6s^2}{c}\,\frac{D_{21} + D_0^{(2)} + 2D_1^{(1)}(C_{21} + C_0^{(2)}) + 2D_2^{(1)}[C_{21} + 4C_{22} + \frac{5}{4}(C_1^{(2)} + C_2^{(2)})]}{1 + 2cs^2A'[2(D_1^{(1)} + D_2^{(1)}) - 1]} \tag{37}$$

and the postbuckling parameter α becomes

$$\alpha = \frac{2}{\pi}\arctan\left[\frac{16}{3S_0(1-16K_cC_{21})}\frac{\lambda_2}{1-\nu^2}\right]. \tag{38}$$

By setting ω and η in all of the above expressions equal to zero the solutions for a corresponding elastic shell are recovered.

RESULTS AND DISCUSSION

Elastic results

In Fig. 3 the results for the critical bifurcation stress of an elastic shell are plotted as a function of the imperfection level $\bar{\xi}$, which is taken to vary from 0 to ∞. The upper curve is the same as the one in [12], except that Koiter's numerical values were calculated with a Poisson's ratio of 0.272, rather than our value of 1/3. It also corresponds to one of the curves in [20] and shows clearly that small imperfections cause a significant reduction of the bifurcation stress. The lower half of Fig. 3 shows that for $\bar{\xi}$ less than about 0.4 (i.e. λ_{cr} greater than about 0.33) α is negative and the initial postbuckling behavior of such a shell is unstable. For larger imperfection levels α becomes positive. In that range the postbifurcation is stable and loads above λ_{cr} can be sustained, i.e. bifurcation does not result in instantaneous loss of load-carrying capacity.

A comparison with the numerical results obtained from an exact buckling and postbuckling analysis [20] (dashed curve) shows good agreement. The values of λ_{cr} agree to within 1%. For α the approximate calculation gives slightly lower values up to approximately $\bar{\xi} = 1$. For larger values of $\bar{\xi}$ the discrepancy is insignificant.

Creep results

Figures 4 show the dependence of the respective critical times on the applied load for various imperfection levels. Consider the curve for $\tilde{\xi} = 0.1$ in Fig. 4(a). The dashed branch gives the critical time τ_a which would be obtained by a purely axisymmetric analysis. The solid branch gives the critical time τ_c for bifurcation buckling. At one point, marked by a solid dot, the two curves merge. It denotes the load level below which no bifurcation will occur and the shell will always collapse axisymmetrically. This transition point existed for all imperfections and creep parameters investigated. Figures 4(b),(c) show similar plots for different parameters of steady and nonsteady creep.

Figure 5(a) shows the relationship between the ratio τ_c/τ_a and λ for steady creep ($n = 3$). It is similar to the ones given by Hoff in [9, 11]. Plots of this kind can be useful in estimating the critical bifurcation time if an estimate of the axisymmetric critical time is available. From Fig. 5(b) it is seen that, except for relatively large imperfections, τ_c/τ_a is almost independent of $\tilde{\xi}$ and is, for all practical purposes, a function of λ/λ_{cr} only.

In Fig. 6 our numerical values for the axisymmetric critical time τ_a are compared with those obtained using Hoff's approximate expression (15). (Recall that the wavelength of the imperfection used by Hoff differs slightly from the one used here.) It is seen that (15) predicts the overall trend but generally overestimates the critical times, especially when λ is small.

Results of the postbuckling analysis are shown in Fig. 7 where the postbuckling parameter α (26) is plotted directly as a function of λ. Consider now Fig. 7(a). First note the dashed curve which represents the elastic results and is obtained from the bottom half of Fig. 3 by eliminating $\tilde{\xi}$. It

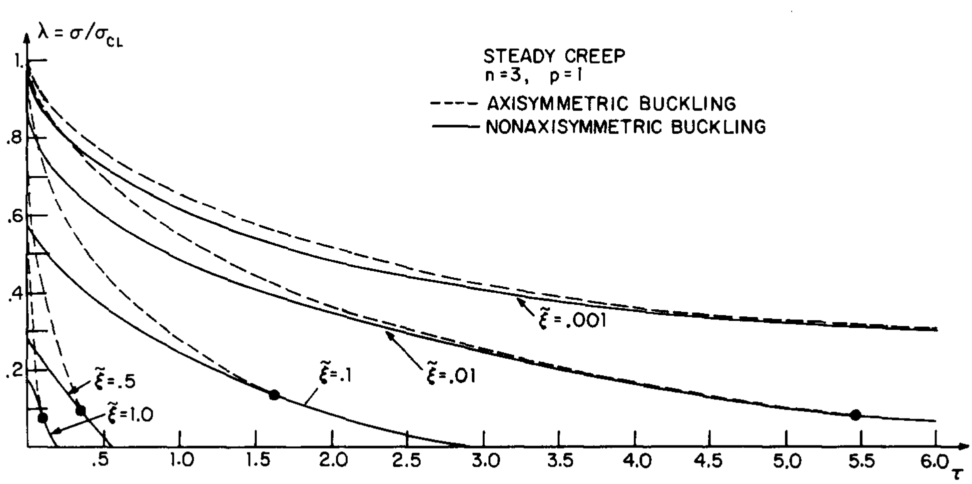

Fig. 4(a). Critical times for imperfect cylindrical shells under axial compression.

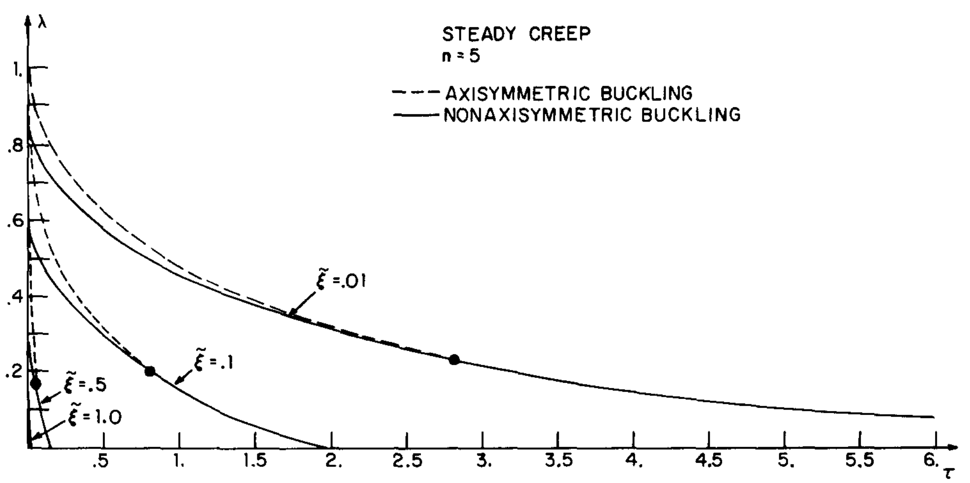

Fig. 4(b). Critical times for imperfect cylindrical shell under axial compression.

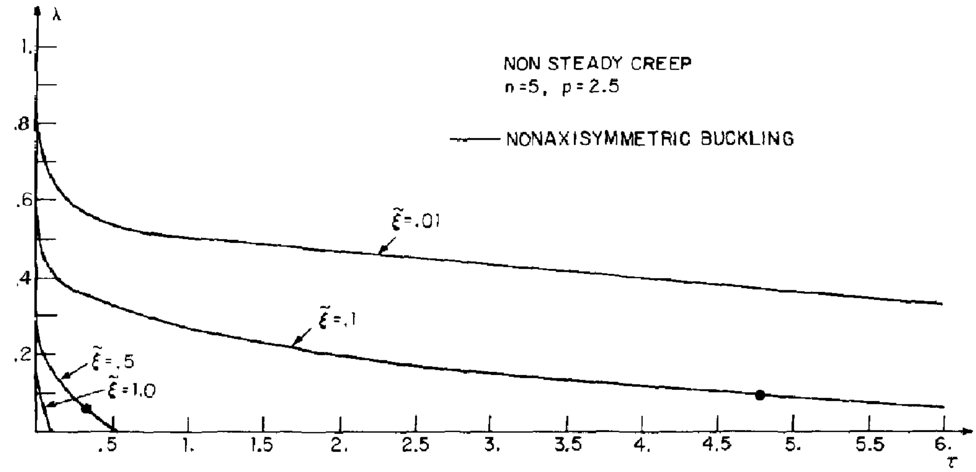

Fig. 4(c). Critical times for imperfect cylindrical shell under axial compression.

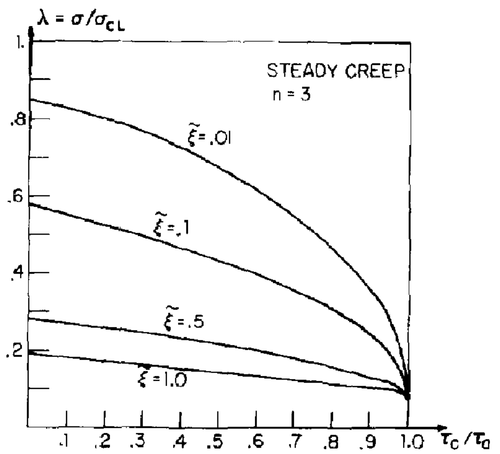

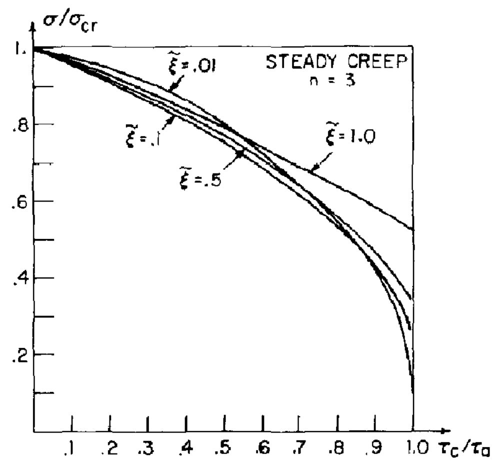

Fig. 5(a). Ratio of nonaxisymmetric to axisymmetric critical times as a function of λ.

Fig. 5(b). Ratio of nonaxisymmetric to axisymmetric critical times as a function of λ/λ_{cr}.

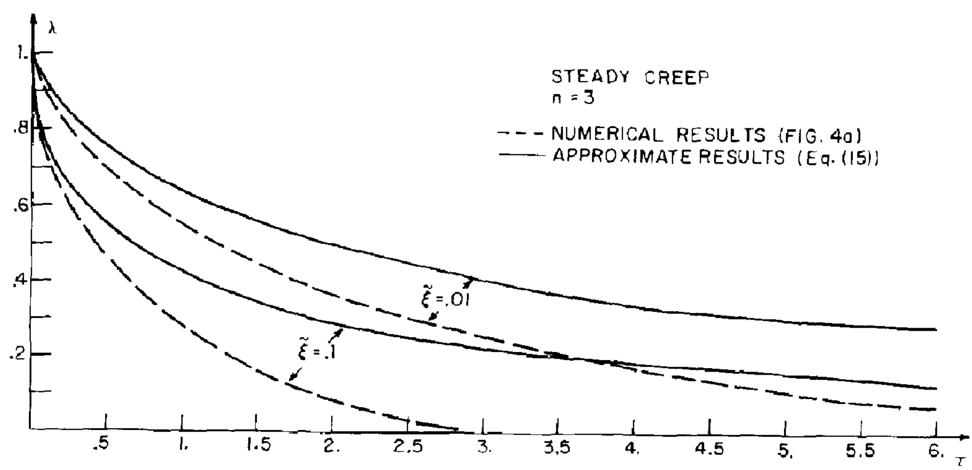

Fig. 6. Comparison of axisymmetric critical times with approximate results.

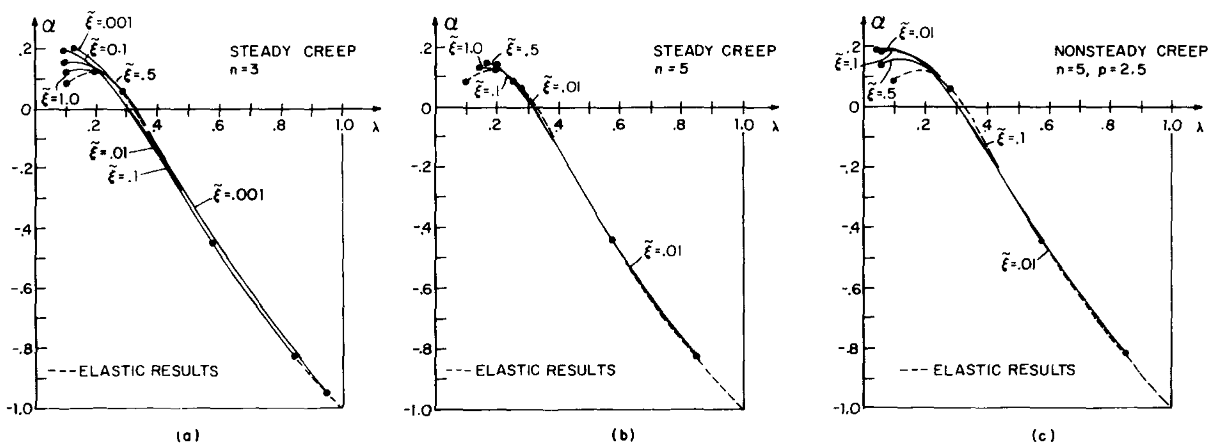

Fig. 7. Postbuckling behavior as a function of the applied stress.

shows the transition from the unstable to the stable postbuckling behavior at a value of λ of about 0.33. The solid dot which terminates the curve at about $\lambda = 0.1$ corresponds to the limit value for $\bar{\xi} \to \infty$. The creep results for various imperfection levels appear in Fig. 7(a) as solid curve-segments. On the left, each starts with a dot at the value of λ below which the shell buckles axisymmetrically (see Figs. 4), and terminates on the elastic curve at the respective value of λ_{cr} (Fig. 3). The composite picture shows clearly that, as far as initial stability or instability is concerned, the postbuckling behavior is strikingly similar to that of an elastic shell and depends essentially only on λ. The transition value between the stable and unstable regions is always approximately $\lambda = 0.3$.

Note from Fig. 3, that for shells with $\bar{\xi}$ greater than about 0.46 the elastic critical load parameter λ_{cr} is smaller than the transition value 0.3. Such shells will have stable initial postbuckling behavior. Note also that α has the largest positive values for small λ. Whereas for an elastic shell this means "more" stability, the same is not necessarily true when the shell creeps. This becomes clear from Fig. 5(a). In the neighborhood of $\lambda = 0.1$ the ratio τ_c/τ_a is close to 1. Thus bifurcation occurs in a range of rapidly increasing displacements, and, in spite of a positive postbuckling stiffness, collapse can be expected shortly after bifurcation.

The same applies to reasonably perfect shells with $\bar{\xi}$ less than about 0.1. For this case Fig. 5(a) reveals that $\lambda < 0.3$ corresponds to $\tau_c \geq 0.8\tau_a$. This means that during a test an observer will probably notice little difference between dynamic snapping and "stable" bifurcation during the phase of rapidly increasing overall displacements. According to this analysis, stable bifurcation and prolonged deformations in the buckled shape would most likely be observed for imperfection levels of about half the thickness (Fig. 5a). The expected creep life would then, of course, be considerably shorter.

Figures 7(a)–(c) show that the main features of the postbuckling behavior are unaffected by the choice of creep parameters.

In the literature it is generally assumed that bifurcation is synonymous with collapse. It was variously presumed that shells with large imperfection wavelengths [4, 8], or with a large value of R/h [18, 3] and/or a moderately high stress level [3] were more likely to bifurcate and collapse. In contrast this analysis indicates that the nature of buckling is completely determined by the value of λ and that R/h plays a role only insofar as it influences the value of λ for a given axial stress σ.

The previous results are summarized in Fig. 2 which has already been explained in the introduction. It is a crossplot of the results of Figs. 4(a) and 7(a). The imperfection level has been eliminated and the critical time is directly related to the applied stress σ and the static buckling stress σ_{cr} of the imperfect elastic shell. If it is assumed that the effect of the imperfections can be judged by the extent to which they reduce the static elastic buckling strength, then plots like Fig. 2 have general validity and $\lambda_{cr} = \sigma_{cr}/\sigma_{c1}$ can be an experimentally or analytically obtained value, or simply a static reduction factor. This would help to eliminate the need for a large number of creep tests.

Plots for the critical circumferential wave number s are not given here. It is only mentioned that it is either close to, or—sometimes considerably—larger than, that of the corresponding elastic shell. Its value decreases with decreasing λ and/or increasing imperfection amplitude.

The close similarities in the buckling behavior of elastic shells and shells undergoing creep have led to approximate bifurcation criteria which are most often based on the assumption that their respective critical radial displacements are identical [11]. It is presumed that the effect of creep is simply to cause the growth of imperfections. This viewpoint neglects, however, the fact that these "new imperfections" are not stress free, and that various deformation histories may produce quite different prebuckling states. In addition, as was mentioned earlier, it is not the prebuckling-displacement, but the curvatures and in-plane stresses, which enter into the buckling problem. Thus a critical-displacement criterion is somewhat arbitrary if the relationship between these quantities is not unique, as is the case in the present creep problem.

This is confirmed by the results shown in Figs. 8. In Fig. 8a the maximum radial displacement w at bifurcation is plotted as a function of λ. The dashed curve shows the same quantity for an elastic shell subjected to the critical bifurcation stress σ_{cr}. At $\lambda = 1$ we have $w = \nu/c$ (see eqn (9)). Figure 8a shows clearly that a critical-displacement criterion leads to very conservative estimates, except for relatively large imperfections. Figure 8b gives the values of the maximum compressive circumferential stress n_{22} at bifurcation. The dashed curve again represents the

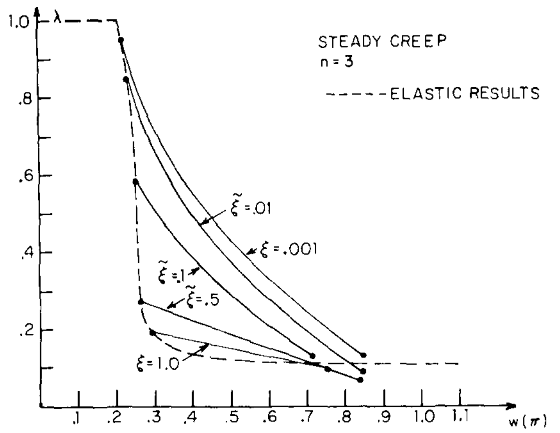

Fig. 8(a). Critical radial displacement as a function of the applied stress.

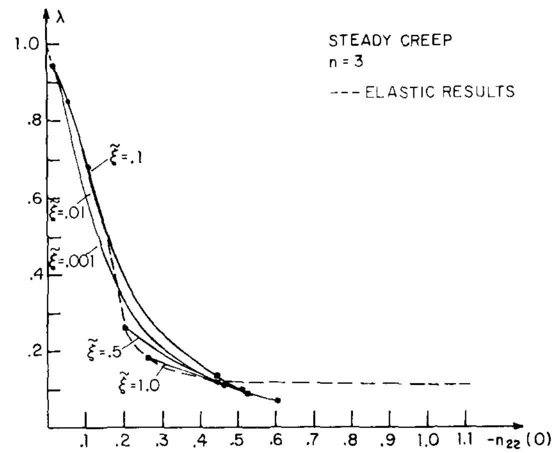

Fig. 8(b). Critical compressive circumferential stress as a function of the applied stress.

critical values for an elastic shell. In this case agreement is much better and Fig. 8(b) yields the, not unexpected, result that the critical circumferential stresses at bifurcation are very nearly equal. An approximate bifurcation criterion based on a critical stress might therefore be expected to give better estimates of the critical time. As in Fig. 8(a) major discrepancies exist around $\lambda = 0.1$. This does not, however, affect the usefulness of such a criterion because in this range bifurcation almost coincides with axisymmetric collapse as discussed above. The results for different values of n and p are quite similar and not given here.

The results of the preceding analysis are qualitatively, and to some extent quantitatively, confirmed by experiments. In tests, metal specimens are usually enclosed in heavily insulated furnaces. They are rarely under continuous observation, and so far the actual process of bifurcation has rarely been observed directly. Samuelson[18] took high-speed photographs which suggest that bifurcation is associated with collapse. But to date only Baranov and Morozov[19] have given an extensive and detailed description of their observations of the buckling behavior of relatively thin aluminum cylinders ($R/h = 116$–197). They note that λ plays an essential role and report three different kinds of buckling and postbuckling behavior. For a Poisson's ratio of 1/3 they observed that for $\lambda > 0.32$ bifurcation resulted in sharp snap-through behavior and a simultaneous drop in the applied load, i.e. unstable behavior. In an intermediate range ($0.32 > \lambda > 0.14$) they report the formation of circumferential buckles, followed by an increase in the rate of deformation and ultimately collapse, i.e. apparently initially stable postbuckling. Finally, for $\lambda < 0.14$ purely axisymmetric buckling was observed. These observations are in complete agreement with the present analysis.

A quantitative comparison of the critical times poses certain problems, since most test reports give critical times but few list all relevant material parameters. Furthermore, as is the case in most shell tests, the magnitude and shape of the imperfections are unknown, and the critical times are usually collapse times. In spite of these qualifications it is felt that a comparison is of value if it can show at least qualitative agreement.

In many respects Samuelson's results[18] are the most complete and they will be used here. The critical times of [18] are nondimensionalized, using the given values $n = 5.8$ and $n = 4.75$. For ν a value of 1/3 was assumed and, to be consistent with Samuelson's assumptions, p was taken equal to 1, although his creep curves indicate that primary creep was always present. The actual critical times varied from 6 to 27,000 min whereas with our nondimensional time parameter they range from 0.1 to 5.

A comparison is now made on the basis of the numerical results for $n = 5$, $p = 1$ and $n = 5$, $p = 2.5$. The experimental results are plotted in Fig. 9 along with the curves from Figs. 4(b),(c) for a very small and a moderate imperfection level, ($\bar{\xi} = 0.01$ and $\bar{\xi} = 0.1$), which presumably represent the range of imperfections, including the effects of the edge disturbance. Considering that creep test results usually show a large amount of scatter the agreement is quite good. For values of λ below the dotted lines labeled I ($n = 5$, $p = 1$) and II ($n = 5$, $p = 2.5$) the analysis predicts axisymmetric buckling. Since the shells which buckled axisymmetrically lie in this range, on this point too, the analysis is in agreement with the test results.

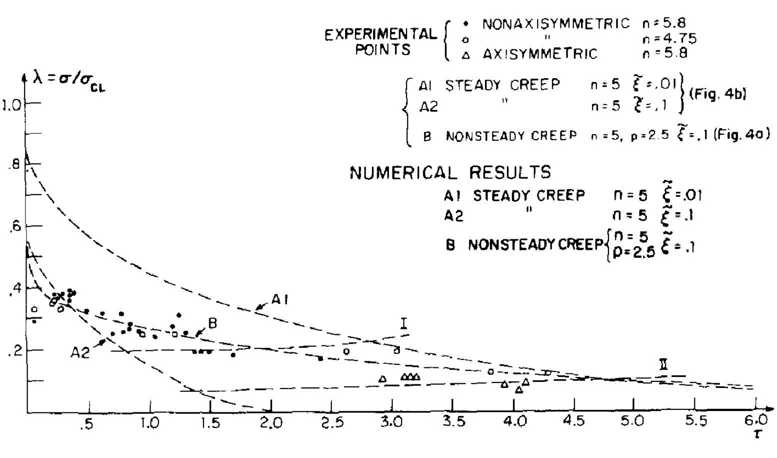

Fig. 9. Comparison with experimental results. (Samuelson[18]).

Samuelson does not mention stable postbuckling behavior. Instead, his high-speed photographs suggest that bifurcation is associated with collapse. From the standpoint of this analysis it can only be said that for $n = 5$, $p = 1$, and the probable imperfection values, the range of λ in which prolonged postbuckling deformations can be expected is quite small, and it is probably quite difficult to distinguish between bifurcation and collapse.

REFERENCES

1. L. Å. Samuelson, A theoretical investigation of creep deformation and buckling of a circular cylindrical shell under axial compression and internal pressure. *FFA Report* 100, The Aeron. Res. Inst. of Sweden, Stockholm (1964).
2. N. J. Hoff, Axially symmetric creep buckling of circular cylindrical shells in axial compression. *J. Appl. Mech.* 35, 530 (1968).
3. L. Å. Samuelson, Creep buckling of a cylindrical shell under non-uniform loads. *Int. J. Solids Structures* 6, 91 (1970).
4. I. M. Levi and N. J. Hoff, Interaction between axisymmetric and nonsymmetric creep buckling of circular cylindrical shells in axial compression. *Proc. IUTAM Symp., Creep in Structures* 1970, *Gothenburg*, 1970 (Edited by J. Hult), p. 405. Springer, Berlin (1972).
5. L. Å. Samuelson, Creep buckling of imperfect circular cylindrical shells under non-uniform external loads. *Proc. IUTAM Symp., Creep in Structures* 1970, *Gothenburg*, 1970 (Edited by J. Hult) p. 388. Springer, Berlin (1972).
6. R. B. Rikards and G. A. Teters, Nonsymmetric creep buckling of cylindrical shells under axial compression and external pressure, *Proc. IUTAM Symp., Buckling of Structures, Cambridge, Massachusetts*, 1974 (Edited by B. Budiansky), p. 78. Springer, Berlin (1976).
7. L. Å. Samuelson, Creep buckling of shells of revolution—User's manual for DSOR 06. *FFA Report HU*-1548, Part 4. The Aeron. Res. Inst. of Sweden, Stockholm (1974).
8. N. J. Hoff, Creep buckling of plates and shells. *Proc.* 13*th Inter. Cong. Theor. Appl. Mech., Moscow*, 1972 (Edited by E. Becker and G. K. Mikhailov), p. 124. Springer, Berlin (1974).

9. N. J. Hoff, Theory and experiment in the creep buckling of plates and shells. *Proc. IUTAM Symp., Buckling of Structures, Cambridge, Massachusetts*, 1974 (Edited by B. Budiansky), p. 67. Springer, Berlin (1976).
10. N. J. Hoff, On the transition from axisymmetric to multilobed creep buckling. *Contributions to the Theory of Aircraft Structures*, p. 297. Delft University Press, Delft (1972).
11. N. J. Hoff, The effect of geometric nonlinearities on the creep buckling time of axially compressed circular cylindrical shells. *J. Appl. Mech.* **42**, 225 (1975).
12. W. T. Koiter, The effect of axisymmetric imperfections on the buckling of cylindrical shells under axial compression. *Proc. Koninkl. Nederl. Akademie van Wetenschappen, Series B* **66**(5), 265 (1963).
13. E. I. Grigoliuk and Y. V. Lipovtsev, On the creep buckling of shells. *Int. J. Solids Structures* **5**, 155 (1969).
14. V. I. Rozenblyum, The snap-through calculation of thin shells in creep. *Izv. AN SSSR MTT* (*Mechanics of Solids*) **4**(3), 79 (1969).
15. G. S. Ganshin, Stability of a cylindrical panel under creep conditions. *Izv. AN SSSR MTT* (*Mechanics of Solids*) **5**(4), 176 (1970).
16. B. Storåkers, Bifurcation and instability modes in thick-walled viscoplastic pressure vessels. *Proc. IUTAM Symp., Creep in Structures* 1970, *Gothenburg*, 1970 (Edited by J. Hult), p. 333. Springer, Berlin (1972).
17. D. Bushnell, Bifurcation buckling of shells of revolution including large deflections, plasticity and creep. *Int. J. Solids Structures* **10**, 1287 (1974).
18. L. Å. Samuelson, Experimental investigation of creep buckling of circular cylindrical shells under axial compression and bending. *Trans. ASME, B, J. Engg. Ind.* 589 (1968).
19. A. N. Baranov and M. A. Morozov, Experimental investigation of the critical strain of cylindrical shells under creep conditions. *Izv. AN SSSR MTT* (*Mechanics of Solids*) **6**(1), 114 (1971).
20. B. Budiansky and J. W. Hutchinson, Buckling of circular cylindrical shells under axial compression. *Contributions to the Theory of Aircraft Structures*, p. 239. Delft University Press, Delft (1972).
21. W. T. Koiter, Over de Stabiliteit van het Elastisch Evenwicht. (On the stability of elastic equilibrium). Thesis, Delft, H. J. Paris, Amsterdam (1945); English translation issued as NASA TT F-10 (1967).
22. Y. N. Rabotnov, *Creep Problems in Structural Members*, p. 210. North-Holland, Amsterdam (1969).
23. J. W Hutchinson, On the postbuckling behavior of imperfection-sensitive structures in the plastic range. *J. Appl. Mech.* **39**, 155 (1972).
24. J. L. Sanders, Jr., Nonlinear theories for thin shells. *Q. Appl. Math.* **21**, 21 (1963).
25. W B. Stephens, Computer program for static and dynamic analysis of symmetrically loaded orthotropic shells of revolution. *NASA TN D*-6158 (1970).
26. M. L. Potters, A matrix method for the solution of a second order difference equation in two variables. *Report MR*19. Mathematisch Centrum, Amsterdam (1955).
27. R. Hill, Bifurcation and uniqueness in nonlinear mechanics of continua. *Problems of Continuum Mechanics* (Edited by J. R. M. Radok), p. 155. SIAM, Philadelphia, Pennsylvania (1961).
28. B. Budiansky and J. W. Hutchinson, Dynamic buckling of imperfection-sensitive structures. *Proc. 11th Inter. Cong. Appl. Mech., Munich*, 1964 (Edited by H. Görtler), p. 636. Springer, Berlin (1966).
29. J. R. Fitch, The buckling and postbuckling behavior of spherical caps under concentrated load. *Int. J. Solids Structures* **4**, 421 (1968).
30. B. Budiansky, Theory of buckling and post-buckling behavior of elastic structures. *Advances in Applied Mechanics* **14**, (Edited by C. S. Yih), p. 1. Academic Press, New York (1974).
31. R. L. Carlson and W. W. Breindel, On the mechanics of column creep. *Proc. IUTAM Coll., Creep in Structures, Stanford University*, 1960 (Edited by N. J. Hoff), p. 272. Springer, Berlin (1962).